Journal of Ecology

British Ecological Society

Journal of Ecology 2011, **99**, 714–723 doi: 10.1111/j.1365-2745.2011.01804.x

SPECIAL FEATURE

ECOLOGICAL CONSEQUENCES OF CLIMATE EXTREMES

Extreme climatic event-triggered overstorey vegetation loss increases understorey solar input regionally: primary and secondary ecological implications

Patrick D. Royer[1,2], Neil S. Cobb[2,3]*, Michael J. Clifford[4], Cho-Ying Huang[5], David D. Breshears[6,7], Henry D. Adams[7] and Juan Camilo Villegas[8]

[1]Columbia Basin Groundwater Management Area, Kennewick, WA 99366, USA; [2]Geospatial Research and Information Laboratory, Northern Arizona University, Flagstaff, AZ 86011, USA; [3]Merriam Powell Center for Environmental Research and Department of Biological Sciences, Northern Arizona University, Flagstaff, AZ 86011,USA; [4]Earth and Environmental Sciences, Lehigh University, Bethlehem, PA 18108, USA; [5]National Taiwan University, Taipei, Taiwan, and Office of Arid Land Studies, University of Arizona, Tucson, AZ 85721, USA; [6]School of Natural Resources and the Environment, University of Arizona, Tucson, AZ 85721, USA; [7]Department of Ecology & Evolutionary Biology, University of Arizona, Tucson, AZ 85721, USA; and [8]Grupo GIGA, Facultad de Ingeniería, Universidad de Antioquia, Calle 57 No.53-108, Medellín, Colombia

Summary

1. Climate extremes such as drought can trigger large-scale tree die-off, reducing overstorey canopy and thereby increasing near-ground solar radiation. This directly affects biotic and abiotic processes, including plant physiology, reproduction, phenology, soil evaporation and nutrient cycling, which themselves affect understory facilitation, productivity and diversity, and land surface–atmosphere fluxes of energy, carbon and water.

2. Although important, assessing extreme-event solar radiation responses regionally following die-off is complex compared with characterizing patch-scale inputs. Estimating regional-scale changes requires integration of broad-scale downward-looking shading patterns due to canopy and topography with fine-scale upward-looking canopy details (e.g. live vs. dead trees, height, diameter, spatial pattern and foliar diffusivity).

3. We quantified increases in near-ground solar radiation following overstorey loss of piñon pine cover in response to a recent extreme drought event (2002–2003). We evaluated 211 km^2 in southwestern USA seasonally and annually using high-spatial resolution satellite imagery, hemispherical ground photography, GIS (Geographic Information System)-based solar radiation modelling tools, *in situ* meteorological data and tree measurements.

4. Overstorey loss due to die-off produced increases in near-ground solar radiation regionally each season – up to 28 W m^{-2}, an increase of 9.1%, in summer – while simultaneously decreasing spatial variation. Annually the increase was *c.* 17 W m^{-2}. Larger increases occurred where initial canopy cover was greater or at higher elevations, by as much as *c.* 80 W m^{-2} (a 40% increase).

5. *Synthesis.* Our results are notable in that they quantify increases regionally in near-ground solar radiation in response to a climate extreme triggering widespread tree die-off. The substantial increases quantified are expected to have primary direct effects on processes such as plant physiology, reproduction, phenology, soil evaporation and nutrient cycling, and secondary effects on understory facilitation, productivity and diversity, and land surface–atmosphere fluxes of energy, carbon and water. Consequently, extreme event-induced changes in near-ground solar radiation need to be considered by both ecologists and physical scientists in assessing global change impacts. More generally, our results highlight an important but sometimes overlooked aspect of plant

---

*Correspondence author. E-mail: neil.cobb@nau.edu

ecology – that plants not only respond to their physical environment and other plants, but also directly modify their physical environment from individual plant to regional scales.

Key-words: climate change, drought, extreme climatic event, Geographical Information System, hemispherical photograph, mesoscale, piñon die-off, plant–climate interactions, QuickBird, remote sensing

Introduction

Climate extremes such as drought, have the potential to rapidly alter vegetation structure and transform associated ecosystem properties (Gutschick & BassiriRad 2003; Gitlin *et al.* 2006; Overpeck & Cole 2006; Jentsch, Kreyling & Beierkuhnlein 2007; Overpeck & Udall 2010; Smith 2011). The consequences of such extreme events can occur rapidly, affecting not only local ecosystems but also entire regions. The ecological impacts of climate extremes are of increasing interest because many regions are projected to experience an increase in the frequency and intensity of climate extremes under global climate change. Of particular concern for the world's globally extensive drylands is the potential for an increase in drought coupled with a warming trend in temperatures (Overpeck & Cole 2006; Jentsch, Kreyling & Beierkuhnlein 2007; McDowell *et al.* 2010; Overpeck & Udall 2010), referred to previously as 'global-change-type drought' (Breshears *et al.* 2005, 2009; Overpeck & Udall 2010). Such global-change-type droughts can represent extreme climatic events (*sensu* Smith 2011), as they have the potential to rapidly and extensively alter vegetation structure due to drought-induced mortality of overstorey plants (McDowell *et al.* 2008; Adams *et al.* 2010). Recently, drought and heat anomalies have been implicated in tree die-off on every wooded continent (Allen *et al.* 2010). Additionally, the effect of warmer temperature has recently been isolated and shown to accelerate drought-induced tree mortality (Adams *et al.* 2009).

An immediate consequence of tree die-off in response to an extreme drought event is a loss in overstorey canopy cover (Allen & Breshears 1998; Royer *et al.* 2010). Substantial loss of overstorey canopy can be viewed as an extreme climatic event (Smith 2011) resulting in the re-ordering of species and possibly the long-term conversion from a woodland to a savanna or grassland. An overstorey loss following tree mortality results in increased near-ground solar radiation, a fundamental driver of ecological processes (Fig. 1). In drylands, tree canopy cover plays a particularly important role in modifying and ameliorating the near-ground solar radiation below the canopy (Scholes & Archer 1997; Breshears 2006). With overstorey loss, increased near-ground solar input has a number of important primary direct ecological effects, including altered physiological processes (Callaway *et al.* 1996; Maestre, Bautista & Cortina 2003; Breda *et al.* 2006), phenology (Breda *et al.* 2006; Rich, Breshears & White 2008), reproduction (Callaway 1992; Chambers, Vander Wall & Schupp 1999; Suarez & Kitzberger 2008), soil evaporation (Breshears *et al.* 1998; Huang *et al.* 2010; Villegas *et al.* 2010a) and nutrient cycling (Padien & Lajtha 1992; Selmants & Hart 2008; Wang *et al.* 2009). The secondary effects of these primary direct effects can be manifested at multiple spatial scales (Notaro, Liu & Williams 2006; Rich, Breshears & White 2008; Huang *et al.* 2010; Royer *et al.* 2010). Among the most notable consequences are reduced understory facilitation (Callaway 1992; Scholes & Archer 1997; Maestre, Bautista & Cortina 2003; Brooker *et al.* 2008; Cingolani *et al.* 2010), decreased productivity and diversity

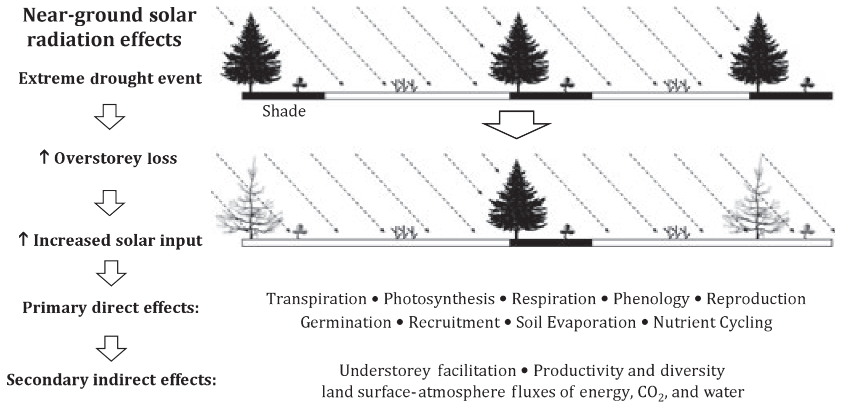

Fig. 1. A conceptual framework for considering the effects and consequences of increased near-ground solar radiation in response to an extreme drought event. Extreme drought events trigger a loss of overstorey canopy cover through drought-induced tree mortality. Overstorey loss leads to increased solar input at the land surface through a loss of shaded patches. Increased near-ground radiation will directly affect understory plant physiology, phenology and reproduction, as well as bare-soil evaporation and nutrient cycling. Specifically, increases in transpiration, respiration, phenological response to spring and soil evaporation, as well as decreases in photosynthesis, reproduction, germination, recruitment and nutrient cycling are expected for a semiarid ecosystem. These direct effects of increased solar input have secondary consequences at multiple spatial scales, including reduction in facilitation of understory plants, decreased primary productivity and species diversity, and alterations to land surface–atmosphere fluxes of energy, CO_2 and water.

(Sthultz, Gehring & Whitham 2007; Butterfield 2009; Madrigal-Gonzalez *et al.* 2010; Zhao & Running 2010) and altered land surface–atmosphere fluxes of energy, carbon and water (Field *et al.* 2007; Bonan 2008; Chapin *et al.* 2008; Adams *et al.* 2010; Anderson *et al.* 2010; Rotenberg & Yakir 2010). Therefore, it is important to better understand the effects of canopy loss on surface energy inputs in order to enable the assessment of these primary and secondary implications.

Several recent studies have quantified trends in solar radiation as a function of woody plant canopy cover, but these studies are primarily focused on local or stand scales, and not on regional scales. Field studies have found that in undisturbed semiarid woodlands, an approximate 50% reduction in near-ground radiation can be expected when moving from 5 to > 60% woody (i.e. trees and shrubs) canopy cover (Royer *et al.* 2010; Villegas *et al.* 2010b) and an up to 80% reduction when including the interactive effects of slope and aspect (Zou, Barron-Gafford & Breshears 2007). Regional patterns of near-ground incoming solar radiation, in addition to varying seasonally (Breshears *et al.* 1997; Villegas *et al.* 2010b), are predominantly determined by topography (Zou, Barron-Gafford & Breshears 2007), amount and spatial pattern of overstorey woody plants, and by their associated foliar diffusivity (Rich *et al.* 1994, 1999; Martens, Breshears & Meyer 2000; Villegas *et al.* 2010a,b). Estimating how such regional patterns would change in response to die-off of overstorey woody plants is challenging because it requires simultaneous consideration of broader-scale topography shading patterns, associated with a digital elevation model (DEM), and finer-scale details of canopy structure including differentiating live from dead trees and factoring in their height, diameter, spatial pattern and foliar diffusivity.

Here, we synthesized data from ground-based measurements and satellite imagery to model the change in near-ground solar radiation that resulted from a recent regional die-off of piñon pine in south-western USA. This widespread tree die-off occurred during a ‘global-change-type drought’, in which warmer temperatures accompanied an extreme drought event and amplified mortality (Breshears *et al.* 2005, 2009), and thus it provides a mesoscale-level (few to several hundred square kilometres) assessment of what vegetation changes we might potentially expect in the rest of the 21st century for drylands with warming climates. We discuss how estimated changes in near-ground solar radiation should have primary direct effects on processes such as plant physiology, reproduction, phenology, soil evaporation and nutrient cycling, and the expected associated secondary effects on understory facilitation, productivity and diversity, and land surface–atmosphere fluxes of energy, carbon and water.

Materials and methods

STUDY AREA

The study area encompassed a 211-km^2 area of the piñon–juniper ecosystem (0.17% of the piñon–juniper ecosystem along the entire Colorado Plateau) located on the north side of the San Francisco Peaks in northern Arizona, USA (Fig. S1 in Supporting Information). Elevations ranged from 1500 to 2450 m a.s.l., average monthly maximum temperature is 24 °C, average monthly minimum temperature is 0.4 °C and average annual rainfall is 280 mm. Evapotranspiration rates are high, at *c.* 410 mm year^{-1}, and precipitation is higher than evapotranspiration only from December to February (Fig. S1). Topographic relief is moderate (although isolated steeper slopes and several small cinder cones have slopes that reach 70°) with an average, but highly variable, north-west aspect (48°). Canopy cover ranges from low open savanna-like physiognomy (< 2% tree canopy cover) to dense interlocking canopy. Spatial heterogeneity of trees can be described as aggregated at a linear distance of < 0.3 km, and completely spatially random from 0.3 to 2 km, based on preliminary multidistance spatial cluster analysis. See Table S1 for a description of tree characteristics, slope, aspect and elevation for the study area, and Fig. S2 for monthly solar radiation, temperature, precipitation and relative humidity.

STEPS IN THE SPATIAL ANALYSIS

We estimated changes in near-ground solar radiation following piñon mortality as a four-step process (Fig. S3). First, we used high-spatial-resolution satellite QuickBird imagery (DigitalGlobe Corporate, Longmont, CO, USA) to calculate tree cover both before and after die-off throughout the study area. Second, we applied canopy height values to the tree-cover estimates provided by QuickBird imagery using ground-based measurements collected from plots that spanned the study area to interpolate across the imagery data. Third, we calculated incoming radiation using processed QuickBird imagery from step 2 and a DEM with solar radiation modelling software, which accounted for topographic variation and atmospheric diffusivity, but did not incorporate tree diffusivity (i.e. tree canopies were treated as solid objects). Fourth, we calculated solar radiation from an upward perspective beneath tree canopies, which attenuate and diffuse radiation, by using hemispherical photographs (Anderson 1964) taken from plots and then applied to the modelled data from step 3. Each of these steps is described below in detail. This four-step process was completed twice: once with pre-mortality tree cover and again with post-mortality tree cover. We obtained data for each month allowing evaluation of seasonal and annual differences in solar radiation following tree die-off.

QUANTIFYING TREE CANOPY COVER AND HEIGHT

We quantified change in total tree cover using 2004 post-die-off high-spatial-resolution QuickBird imagery. The sensor collects one panchromatic (spectral range: 450–900 nm) and four multispectral images [blue band: 450–520 nm, green: 520–600 nm, red: 630–690 nm, near-infrared (NIR): 760–900 nm]. The dynamic range of the imagery is 11 bit, and the spatial resolutions are 0.61 and 2.44 m at nadir for the panchromatic and multispectral imageries, respectively. The imagery was collected on 2 June 2004 at 18:13:20 UTC. We quantified live tree canopy, dead tree canopy and intercanopy areas by performing a supervised classification with the satellite imagery, creating 125 ‘training sites’ based primarily on the NIR band in pixel clusters using ERDAS v 9.1 image analysis software (ERDAS Inc., Atlanta, GA, USA). We applied the results of our supervised classifications to the entire imagery to determine the presence of live and dead trees; the combination of both live and dead was used as an estimation for total tree cover before die-off, and only live trees were used as tree cover after tree die-off. Classifications were ground-truthed by comparing percentage canopy cover estimates collected in the field in 2002 (pre-mortality) and 2004 (post-mortality) with percentage canopy cover estimates from the pre- and post-mortality classifications, respectively. Comparisons between field and remotely sensed data were made in 18 randomly established transects (Floyd *et al.* 2009). Raster images were masked to include the transect polygons and canopy cover was obtained from classifications of QuickBird within each belt transect. Canopy cover classifications derived from both pre-drought ($r^2 = 0.803$) and post-drought ($r^2 = 0.806$) exhibited strong correlation with ground-based observations. We were able to detect dead canopies because most of the fine branches and some needles were present, thus distinguishing dead trees from other objects.

To estimate tree height, we obtained data from 842 10 × 10 m plots from pre-existing belt transects randomly distributed throughout the study area. The data from > 4300 individual trees were summarized as follows: average tree height ± SD was 2.61 ± 2.99 m, average basal area was 3430.07 ± 4651.80 cm^2 100 m^{-2}, average tree density was 2.72 ± 2.13 individuals 100 m^{-2}, average crown diameter was 2.20 ± 0.68 m and average canopy cover was 16.44 ± 10.83 m^2 100 m^{-2}. The mean tree height data were interpolated over the extent of the study area using inverse distance weighting (IDW). The root mean-squared error of IDW was 0.43 m with the uncertainty of 16.46%; the mean prediction (2.58 m) was very close to field observation (2.61 m) with a deviation of 1.18%. The tree height was spatially correlated (Moran's $I = 0.35$, $P = 0.001$) (Space-Time Intelligence System; TerraSeer Technology, Ann Arbor, MI, USA), which justifies the use of IDW.

'TOP-DOWN' AND 'BOTTOM-UP' ESTIMATES OF NEAR-GROUND SOLAR RADIATION

Global radiation above tree canopies is the sum of direct, diffuse and reflected radiation. Near-ground solar radiation is the amount of total radiation that arrives at the ground surface (< 1 m above surface) after accounting for the additional attenuation of solar radiation by plant canopies. For our 'top-down' estimation of solar radiation, we used ArcMap v. 9.3 (ESRI Inc., Redlands, CA, USA) Area Solar Radiation spatial extension with a DEM of our study area. The solar radiation tool accounts for site latitude, slope, aspect and daily shifts in the sun angle, enabling one to map and analyse insolation of a geographic area for a specific time period. Calculations for a geographic area are made by overlaying a viewshed on a direct sunmap to estimate direct radiation, and overlaying a diffuse skymap to estimate diffuse atmospheric radiation. The process is repeated at every pixel, accounting for an upward-looking viewshed based on topography. We re-sampled 10-m DEMs to 1-m resolution using bilinear interpolation and calculated near-ground solar radiation to the extent of the QuickBird Imagery. The solar radiation utility allows for control of diffusivity using a dimensionless ratio of 0.0 to 1.0 to simulate cloud cover, and we calibrated our model seasonally and annually by averaging solar radiation data between 2003 and 2009 from a meteorological station located centrally in our study area (Northern Arizona University, C. Hart Merriam Elevation Gradient, 35.50, -111.62).

To account for near-ground radiation directly under trees and in the contiguous intercanopy areas, which could not be evaluated in our 'top-down' aerial GIS (Geographical Information System) model, we acquired 'bottom-up' images with a digital camera (Nikon Coolpix 5400; Nikon Corporation, Tokyo, Japan) fitted with a 10.5-mm Nikkor fisheye lens (Nikkor FC-E9; Nikon Corporation) on a self-levelling mount. We used Hemiview Canopy Analysis v. 2.1 (Delta-T Devices Ltd, Cambridge, UK) to calculate solar radiation below tree canopies. Our approach using hemispherical photographs enabled us to account for attenuation of light underneath tree canopies, essentially becoming the 'bottom-up' solar radiation counterpart of the 'top-down' solar radiation model. To calculate solar radiation directly below tree canopies, we took a photo at each cardinal direction below tree canopies, midway between the base and canopy edge, and averaged values. To estimate the shading affect of trees of various heights in the intercanopy, we took 10 photographs, each one at 1-m intervals moving from the canopy edge into the intercanopy in the shaded cardinal direction: north, east and west (total of 30 intercanopy photos for each tree). We repeated our canopy photos and intercanopy photos for trees < 2, 2, 3, 4 and 5 m tall in each major height class of our study area. Applying data from trees of different height allowed us to account for obvious differences of shaded length and shaded fraction in intercanopy areas, as well as for variation in shade directly beneath trees as a consequence of variation in total foliage correlated with increasing tree height.

Our final pre- and post-die-off maps were created by merging our top-down regional modelled solar radiation results with our 'bottom up' solar radiation estimates below tree canopies. We overlaid original solar radiation maps from DEMs with tree canopies that were classified from satellite images to establish the presence of cover. Where trees were present, we systematically converted pixels from 'top-down' solar radiation values derived from the model to their respective 'bottom-up' canopy radiation value, and intercanopy solar radiation values derived from hemispherical photographs based on tree height. We repeated these steps on monthly and annual integrals for both the 'top-down' and 'bottom-up' techniques to obtain seasonal and annual trends, allowing us to calculate the exact shaded fraction and shaded pixels for trees of various heights in the contiguous area around each tree. We accounted for mutual shading, by either coalescing shade from nearby trees or the shade from a slope imposed over the shade of a tree, with a raster calculation conditional statement that set shaded value equal to the lowest radiation value where mutual shading occurred. In determining near-ground radiation following die-off, tree canopies classified as dead were considered to be open intercanopy areas, void of any direct tree cover, and removed from subsequent calculations. Although standing dead trees do attenuate a small amount of direct beam radiation (Suarez & Kitzberger 2008; Royer *et al.* 2010), dead piñon snags fall within 10 years, and all needles and most finer branches fall within 2 years following death (Clifford *et al.* 2008).

DATA ANALYSIS

We examined the general effect of die-off on near-ground radiation for each season (using the month with a solstice or an equinox) and for an annual integration across all months, and evaluated the finer-scale responses as a function of tree cover. Because the novelty of our approach involved simultaneous consideration of broad-scale topographic patterns in concert with patch-scale canopy loss, we evaluated the effect of mortality with potentially significant biophysical covariates. Additionally, we characterized the effects of die-off on variance of near-ground radiation. To compare our final solar radiation values before and after die-off in the context of the specific aforementioned objectives, we generated random 5-ha circular subplots ($n = 165$) nested within the study site, and derived mean and spatial variance for near-ground solar radiation in each subplot. Based on statistical sampling theory, the number of random plots within our study area ($n = 165$) provides a certainty of $> 90\%$ for representing the mean and variation for the extent of our study area (Yamane 1967). We chose a random sampling design to evaluate our data, because inherent spatial autocorrelation of remotely sensed data prevents the use of regular statistical tests (Isaaks & Srivastava 1989). Therefore, it is necessary to sample the data randomly to create independence (Gruijter & Braak 1990; Brus & DeGruijter 1993). In order to account for individual trees, we developed our data on a 1-m^2 pixel-by-pixel basis; however, we evaluated our results by aggregating and averaging values at the 5-ha plot size. The larger plot size reflects a spatial resolution that approximates field studies in near-ground solar radiation in semiarid woody systems (Zou, Barron-Gafford & Breshears 2007; Royer *et al.* 2010; Villegas *et al.* 2010b) and atmospheric flux response following disturbance in conifer-dominated studies (Suarez & Kitzberger 2008; Montes-Helu *et al.* 2009).

We calculated the average change in mean radiation and variance annually and seasonally (in January, March, June and September) and used a paired *t*-test to compare near-ground radiation before and after die-off at each season and annually. To evaluate the effect of cover alone, we grouped pre-mortality canopy cover into observed cover classes of low, medium and high levels (0–5%, 6–14% and $> 14\%$ canopy cover, respectively), and used a two-way analysis of variance to test for the effect on near-ground radiation of both (i) tree cover classes and (ii) die-off. We used stepwise forward regression to determine significant explanatory variables (percentage slope, aspect, elevation, percentage canopy loss, and the interaction between elevation and canopy loss) on annual differences in near-ground radiation following die-off to identity significant covariates and develop the most parsimonious model. We converted aspect from degrees to a continuous linear range of 0 on north-eastern slopes (receiving the lowest amount of direct radiation), to 1 on south-western slopes (receiving the highest amount of direct radiation). No other covariates were transformed from their original units. In each plot ($n = 165$) we calculated variance in near-ground solar radiation corresponding to canopy cover, for both pre-die-off and post-die-off, and graphed the results as a second order function.

Results

ANNUAL AND SEASONAL CHANGES IN NEAR-GROUND RADIATION

Canopy cover decreased from 13.5% in 2002 to 5.8% in 2004 during the period corresponding to massive drought-induced mortality throughout the study area (Fig. 2). Even though much of the region had low pre-die-off tree canopy cover typical of woodlands, the change in canopy cover due to the die-off was substantial enough to produce a regional-scale average annual increase in seasonal near-ground solar radiation of 17 W m^{-2}, a *c.* 10% increase ($P < 0.01$; Fig. 3). Increases in

(a) Pre-die-off tree cover

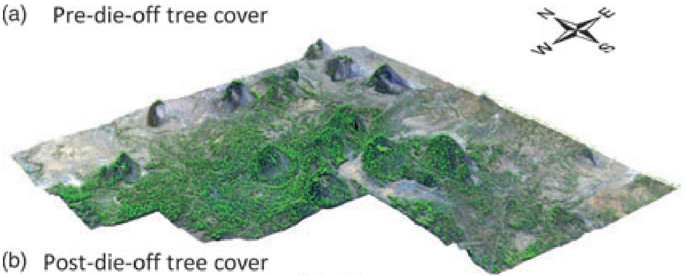

(b) Post-die-off tree cover

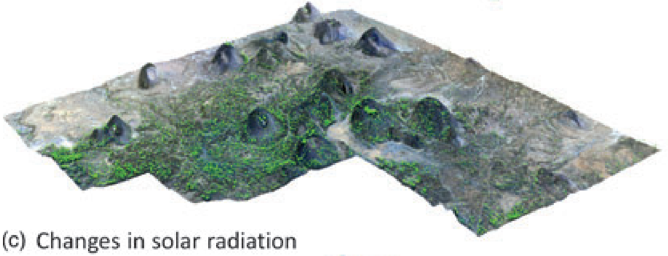

(c) Changes in solar radiation

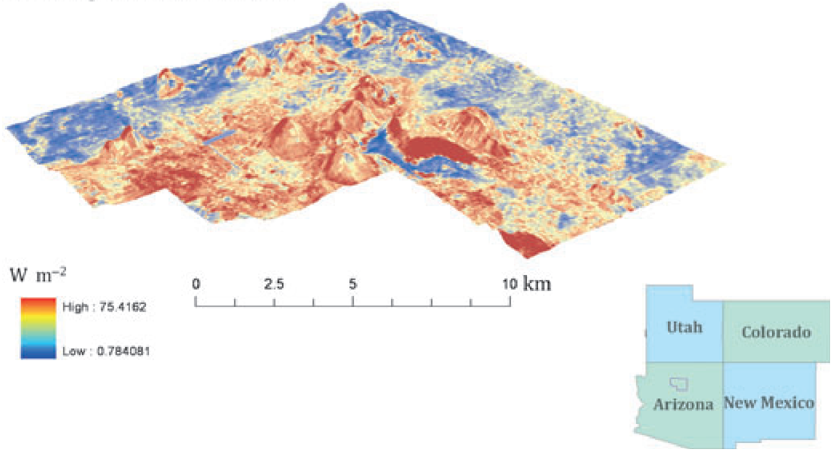

Fig. 2. Regional-scale changes in near-ground radiation following die-off, depicting initial tree cover (a), tree cover following die-off (b) and resulting changes in near-ground solar radiation (c). Modelled results shown here were re-sampled to a much coarser resolution from the original 1-m resolution for smoothness and clarity, thus the scale *c.* 0–75 W m^{-2} in the figure reflects the averaging of results over coarser sample size.

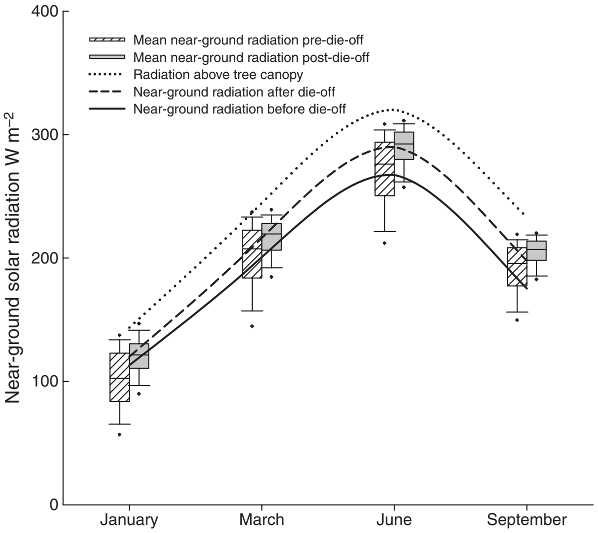

Fig. 3. Seasonal differences in total near-ground solar radiation before and after die-off normalized by global radiation values from weather stations in piñon–juniper shown depicted with monthly means as calculated from the 165 subplots, 25–75% confidence intervals (whiskers) and 5–95% confidence intervals (outlying dots). Mean seasonal interpolated trend lines for above canopy global radiation (dotted line), near-ground radiation after die-off (dashed line) and near-ground radiation following die-off (solid line). Near-ground solar radiation increases in each season (all P-values < 0.01) and as an annual average ($P < 0.01$).

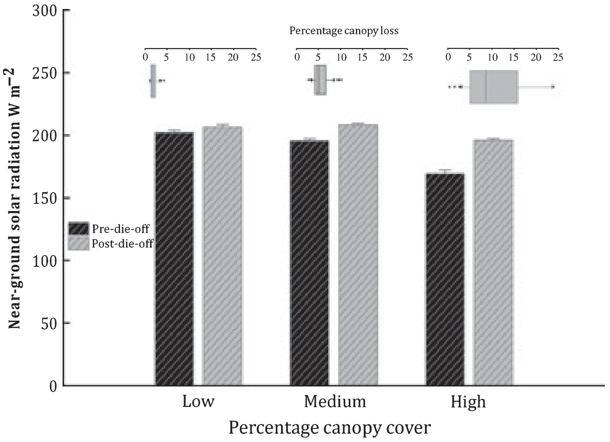

Fig. 4. Mean annual solar radiation before and after die-off for low (0–5% canopy), medium (5–14% canopy) and high canopy (15–50% canopy) total woody cover. Each bar represents the annual average near-ground solar radiation before (white checked boxes) and after (solid grey boxes) die-off, shown with the standard error of the mean (SE) for fifty-five 5-ha subplots in each canopy classification. Annual variation in near-ground solar radiation decreases after die-off as a general trend ($P < 0.01$), and at each canopy level ($P < 0.01$). Inset horizontal box plots above reflect the percentage absolute canopy die-off in each cover class, depicted with 95% confidence intervals and outliers.

near-ground solar radiation were most pronounced in spring (March) and summer (June), when average radiation increased by 25 W m^{-2} ($P < 0.01$) and 29 W m^{-2} ($P < 0.01$), respectively (Fig. 3).

SOLAR RADIATION CHANGES ACROSS CANOPY COVER CLASSES

In addition to the affect of seasonality, we found that increases in solar radiation were significantly affected by general canopy cover classes (low, medium and high; $P < 0.001$). Differences in near-ground solar radiation were significant between every canopy class (Tukey's honest significant difference), even though a large proportion of the overall significance was explained by the difference between high canopy cover vs. combined low and medium cover values (F-ratio = 178, linear contrast; Table S2 and Fig. 4). The annual changes in subplots with high amounts of initial woody plant cover (15% and greater) were greatest where near-ground radiation increased consistently by an average of 30 W m^{-2}. Conversely, increases in radiation were muted in areas of low canopy cover (5% and less), increasing by an average of only 4 W m^{-2} (Fig. 4). Increases in near-ground radiation rivalling 75 W m^{-2} were observed in plots where die-off was most pronounced, highlighting that local changes can exceed the estimated regional increases by a factor of 4 (Fig. 5). We also found that pre-die-off canopy cover was proportional to the absolute percentage loss of canopy cover ($P < 0.01$; Fig. 4); however, relative canopy cover loss (the percentage canopy cover loss relative to the amount of pre-die-off canopy cover) was not correlated with the amount of initial canopy cover.

SOLAR RADIATION CHANGES WITH CANOPY LOSS AND ELEVATION

Step-wise regression was used to examine the influence of percentage canopy die-off and biophysical covariates on changes in near-ground radiation. This analysis indicated that the most parsimonious model following die-off included only mean elevation and absolute canopy die-off (Table S3 and Fig. 3). After accounting for the effect of canopy loss, near-ground solar radiation increased by an average of 0.05 W m^{-2} with each metre increase in elevation. Generally, near-ground solar radiation increased by an average of 27 W m^{-2} at elevations >2200 m a.s.l., and increases were muted at the lowest elevations in our study site, where the change was <5 W m^{-2}. The increase in the plot mean for regional near-ground solar radiation was accompanied by a decrease in spatial variance among subplots within the region (Fig. 6), resulting in a larger and more homogenous energy input term. We observed an overall decrease in variation associated with cover reduction at low and intermediate canopy cover values, and a complete loss of canopy accounting for areas that exceeded *c.* 28% cover (Fig. 6).

Discussion

CHANGES IN NEAR-GROUND SOLAR RADIATION FOLLOWING DIE-OFF

Our results are notable in that they quantify plant-induced increases in near-ground solar radiation in response to

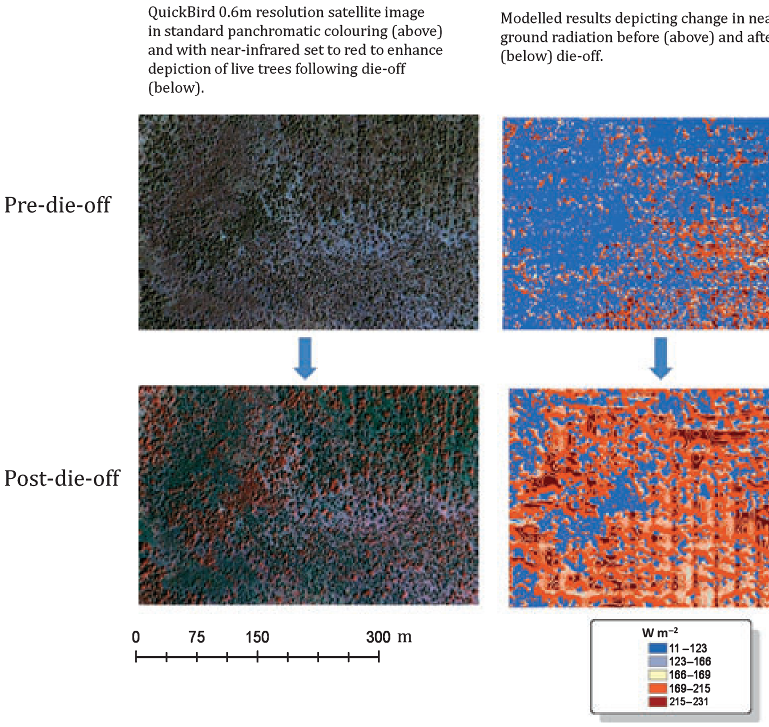

Fig. 5. Pre- and post-die-off depiction of decrease in canopy cover and resulting near-ground solar radiation. Initial (pre-die-off) panchromatic representation of 0.61 m Quickbird imagery and resulting near-ground radiation. Post-die-off classification illustrating classification technique, where the near-infrared (NIR) band is assigned a red value, and the RGB imagery clearly outlining areas of tree survival (red, high NIR reflectance) and tree mortality (areas with low NIR signals). Canopy decreased by 53% and average annual near-ground solar radiation increased by 50.47 W m^{-2} (30% increase in solar radiation; $P < 0.01$).

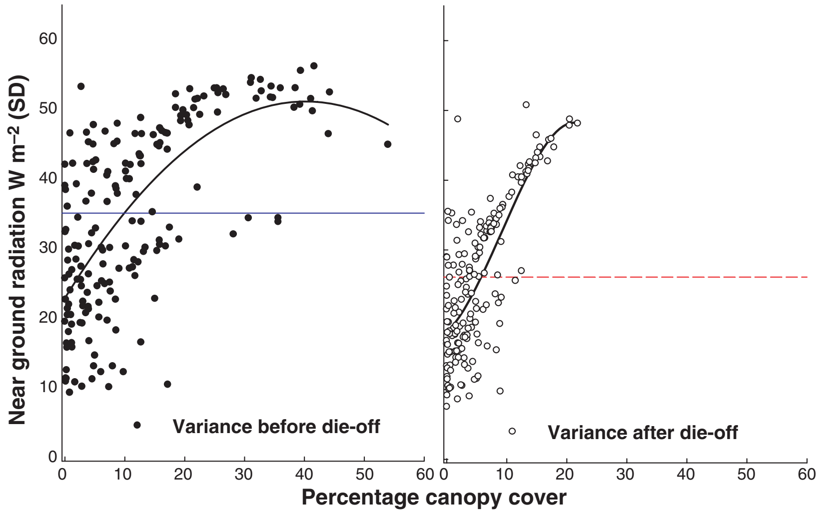

Fig. 6. Comparison of variance in near-ground radiation at the site scale as a function of canopy cover before and after die-off. Each point represents the variance within a 5-ha plot at a specified level of canopy cover.

regional-scale vegetation change from drought-induced tree mortality. Our results also quantify how the increases in near-ground solar radiation varied seasonally and with amount of tree cover, after accounting for variation associated with elevation. The study area, which encompassed 211 km^2, spanned from lower-elevation savanna vegetation to higher-elevation dense woodland and included variation in tree cover and elevation typical of piñon–juniper woodlands on the Colorado Plateau. The scale of our study, in conjunction with other studies (Breshears *et al.* 2005; Shaw, Steed & DeBlander 2005; Floyd *et al.* 2009; Huang *et al.* 2009), provides an estimate that could be relevant for the larger 130 000 km^2 of piñon–juniper woodlands on the Colorado Plateau.

Our approach expands on other studies carried out at plot-to-stand scales that have focused on identifying trends along canopy gradients using only hemispherical photography (Zou, Barron-Gafford & Breshears 2007; Breshears & Ludwig 2010; Royer *et al.* 2010; Villegas *et al.* 2010b; Zou, Royer & Breshears 2010). We build on these studies to quantify regional response based on a synoptic approach of an aerial-based large-scale 'top-down' model. The results are consistent with previous density-dependent relationships quantified for piñon–juniper woodlands (Royer *et al.* 2010), and changes with amount of tree cover were evident, even though much of the study area encompassed low-density stands. Our results reflect the interactive effects of topography (elevation, slope, aspect) with canopy cover, consistent with Zou, Barron-Gafford & Breshears (2007), although the interrelationships were more muted for the actual topography that we studied in contrast to the simple topographic planes used in that previous study. Our analyses isolated elevation effects on solar radiation, allowing us to more fully evaluate changes associated with tree cover pre- and post-die-off. In addition, our results on how spatial variance in near-ground solar radiation depends on the amount of canopy cover are also consistent with previous findings. We found a peak variance in solar radiation before die-off at between 30% and 40% canopy cover (Fig. 6), similar to findings from studies that used hemispherical photography alone (Royer *et al.* 2010; Villegas *et al.* 2010b) or that modelled solar radiation treating trees as ellipses (Martens, Breshears & Meyer 2000). Following die-off, plot-scale variance was truncated at 20% canopy cover at which variance was the greatest, consistent with general trends in variance following die-off estimated using hemispherical photographs alone (Royer *et al.* 2010).

CONSEQUENCES OF DIE-OFF-INDUCED OVERSTOREY VEGETATION LOSS

Our analyses quantify substantial changes in near-ground solar radiation, which are large enough that their primary direct effects should not be overlooked (Fig. 1). Physiological processes such as photosynthesis are very sensitive to changes in understory light (Pearcy *et al.* 1990), so our estimated changes of as much as 75 W m^{-2} are likely to have direct physiological effects. This near-ground radiation increase is also consistent with observed and expected shifts in phenological responses towards an earlier green-up of understory vegetation and greater amplitude between peaks and troughs of green-up annually (Rich, Breshears & White 2008). Given that germination and establishment rates for piñon reproduction are highly temperature- and shade-sensitive, the increased near-solar radiation likely directly affects these processes (Emerson 1932; Meagher 1943; Everett, Koniak & Budy 1986; Chambers, Vander Wall & Schupp 1999). In addition, soil evaporation is affected by near-ground solar radiation input and associated soil temperature (Breshears *et al.* 1998) and is expected to increase in response to overstorey loss following die-off. Decomposition rates depend more directly on soil moisture than temperature in piñon–juniper woodlands (Conant *et al.* 1998, 2004), but the increases in incoming solar radiation beneath formerly live canopies that we quantified could directly increase decomposition rates due to increased UV photodegradation (Austin & Vivanco 2006; Austin & Ballare 2010).

The expected secondary effects from this suite of likely primary direct effects are at least threefold (Fig. 1). First, facilitation is increasingly being recognized as an important process structuring communities (Brooker *et al.* 2008; Brooker & Callaway 2009; Maestre *et al.* 2009; Madrigal-Gonzalez *et al.* 2010), and overstorey shading plays an important role in facilitation of understorey plants in semiarid ecosystems (Callaway 1992; Maestre, Bautista & Cortina 2003; Sthultz, Gehring & Whitham 2007); therefore the direct effects on shading that we quantify could well affect facilitation relationships in these woodlands (Emerson 1932; Meagher 1943; Everett, Koniak & Budy 1986; Chambers, Vander Wall & Schupp 1999). Second, productivity and diversity can also be affected by the reduced facilitation associated with increased near-ground solar input (Sthultz, Gehring & Whitham 2007; Butterfield 2009; Madrigal-Gonzalez *et al.* 2010) and changes in phenology such as those we describe can be interrelated with productivity (Rich, Breshears & White 2008; Davison *et al.* 2011). Third, clearly near-ground solar radiation can alter land surface–atmosphere fluxes of energy, carbon and water – overstorey vegetation loss directly affects incoming near-ground solar radiation, thereby influencing ecologically important exchanges of mass and energy, including evapotranspiration (latent heat exchange), convection, sensible heat transfer, ground heat fluxes and C fluxes (Charney *et al.* 1977; Bonan 1997, 2008; Anderson *et al.* 2010; Raz-Yaseef, Rotenberg & Yakir 2010). Notably, the magnitude of changes in near-ground solar radiation that we quantify is of similar degree to those associated with Amazon deforestation that resulted in increased temperatures (Bastable *et al.* 1993; Eltahir & Humphries 1998; Pongratz *et al.* 2006). This study only quantified the initial response to overstorey loss in terms of changes in near-ground solar radiation and hypothesized expected primary direct effects and their secondary ecological consequences, but we have not quantified those effects and consequences. Additional field and modelling studies are needed to more fully evaluate the potentially cascading ecological consequences of die-off-induced overstorey loss (Smith 2011), but our results nonetheless indicate that these effects and consequences are likely to be substantial.

In conclusion, we quantified regional increases in near-ground solar radiation in response to an extreme event triggering widespread tree die-off. Quantifying these changes in near-ground solar radiation required considering a dual approach using landscape topography looking downward and hemispherical photography from the understory looking upward. Notably, overstorey loss due to die-off produced increases in near-ground solar radiation regionally each season – up to 28 W m^{-2}, an increase of 9.1%, in summer – while simultaneously decreasing spatial variation. These substantial increases are expected to directly affect processes such as plant physiology, reproduction, phenology, soil evaporation and nutrient cycling, and to have more general consequences for understory facilitation, productivity and diversity, and land surface–atmosphere fluxes of energy, carbon and water. In addition, our results are consistent with, and add to, recent conceptual works on the biophysical impacts of forest disturbance and management (Chapin *et al.* 2008; Anderson *et al.* 2010). Consequently, extreme climatic event-induced changes in near-ground solar radiation may need to be more explicitly considered by ecologists as well as physical scientists in assessing global change impacts. More generally, our results highlight an important but sometimes overlooked aspect of plant ecology that plants not only respond to their physical environment and to other plants, but they also directly modify their physical environment from the individual plant to regional scales.

Acknowledgements

This work was supported in part by NSF DEB -0443526 Drought Impacts on Regional Ecosystem Networks (DIREnet), DOE National Institute for

Climate Change Research (Western Region; DE-FCO2-O6ER64159) and Arizona Agriculture Experiment Station. We greatly appreciate the comments of two anonymous referees who provided valuable suggestions that improved the manuscript.

References

Adams, H.D., Guardiola-Claramonte, M., Barron-Gafford, G.A., Villegas, J.C., Breshears, D.D., Zou, C.B., Troch, P.A. & Huxman, T.E. (2009) Temperature sensitivity of drought-induced tree mortality portends increased regional die-off under global-change-type drought. *Proceedings of the National Academy of Sciences of the United States of America*, **106**, 7063–7066.

Adams, H.D., Macalady, A.K., Breshears, D.D., Allen, C.D., Stephenson, N.L., Saleska, S.R., Huxman, T.E. & McDowell, N.G.. (2010) Climate-induced tree mortality: earth system consequences. *Eos*, **91**, 153–154.

Allen, C.D. & Breshears, D.D. (1998) Drought-induced shift of a forest-woodland ecotone: rapid landscape response to climate variation. *Proceedings of the National Academy of Sciences of the United States of America*, **95**, 14839–14842.

Allen, C.D., Macalady, A.K., Chenchouni, H., Bachelet, D., McDowell, N., Vennetier, M. *et al.* (2010) A global overview of drought and heat-induced tree mortality reveals emerging climate change risks for forests. *Forest Ecology and Management*, **259**, 660–684.

Anderson, M.C. (1964) Studies of the woodland light climate. I. The photographic computation of light condition. *Journal of Ecology*, **52**, 27–41.

Anderson, R.G., Canadell, J.G., Randerson, J.T., Jackson, R.B., Hungate, B.A., Baldocchi, D.D. *et al.* (2010) Biophysical considerations in forestry for climate protection. *Frontiers in Ecology and the Environment*, in press doi: 10.1890/090179.

Austin, A.T. & Ballare, C.L. (2010) Dual role of lignin in plant litter decomposition in terrestrial ecosystems. *Proceedings of the National Academy of Sciences of the United States of America*, **107**, 4618–4622.

Austin, A.T. & Vivanco, L. (2006) Plant litter decomposition in a semi-arid ecosystem controlled by photodegradation. *Nature*, **442**, 555–558.

Bastable, H.G., Shuttleworth, W.J., Dallarosa, R.L.G., Fisch, G. & Nobre, C.A. (1993) Observations of climate, albedo, and surface radiation over cleared and undisturbed Amazonian forest. *International Journal of Climatology*, **13**, 783–796.

Bonan, G.B. (1997) Effects of land use on the climate of the United States. *Climatic Change*, **37**, 449–486.

Bonan, G.B. (2008) Forests and climate change: forcings, feedbacks, and the climate benefits of forests. *Science*, **320**, 1444–1449.

Breda, N., Huc, R., Granier, A. & Dreyer, E. (2006) Temperate forest trees and stands under severe drought: a review of ecophysiological responses, adaptation processes and long-term consequences. *Annals of Forest Science*, **63**, 625–644.

Breshears, D.D. (2006) The grassland-forest continuum: trends in ecosystem properties for woody plant mosaics? *Frontiers in Ecology and the Environment*, **4**, 96–104.

Breshears, D.D. & Ludwig, J.A. (2010) Near-ground solar radiation along the grassland-forest continuum: tall-tree canopy architecture imposes only muted trends and heterogeneity. *Austral Ecology*, **35**, 31–40.

Breshears, D.D., Rich, P.M., Barnes, F.J. & Campbell, K. (1997) Overstorey-imposed heterogeneity in solar radiation and soil moisture in a semiarid woodland. *Ecological Applications*, **7**, 1201–1215.

Breshears, D.D., Nyhan, J.W., Heil, C.E. & Wilcox, B.P. (1998) Effects of woody plants on microclimate in a semiarid woodland: soil temperature and evaporation in canopy and intercanopy patches. *International Journal of Plant Sciences*, **159**, 1010–1017.

Breshears, D.D., Cobb, N.S., Rich, P.M., Price, K.P., Allen, C.D., Balice, R.G. *et al.* (2005) Regional vegetation die-off in response to global-change-type drought. *Proceedings of the National Academy of Sciences of the United States of America*, **102**, 15144–15148.

Breshears, D.D., Myers, O.B., Meyer, C.W., Barnes, F.J., Zou, C.B., Allen, C.D., McDowell, N.G. & Pockman, W.T. (2009) Tree die-off in response to global change-type drought: mortality insights from a decade of plant water potential measurements. *Frontiers in Ecology and the Environment*, **7**, 185–189.

Brooker, R.W. & Callaway, R.M. (2009) Facilitation in the conceptual melting pot. *Journal of Ecology*, **97**, 1117–1120.

Brooker, R.W., Maestre, F.T., Callaway, R.M., Lortie, C.L., Cavieres, L.A., Kunstler, G. *et al.* (2008) Facilitation in plant communities: the past, the present, and the future. *Journal of Ecology*, **96**, 18–34.

Brus, D.J. & DeGruijter, J.J. (1993) Design-based versus model-based estimates of spatial means: theory and application in environmental soil science. *Environmetrics*, **4**, 123–152.

Butterfield, B.J. (2009) Effects of facilitation on community stability and dynamics: synthesis and future directions. *Journal of Ecology*, **97**, 1192–1201.

Callaway, R.M. (1992) Effect of shrubs on recruitment of *Quercus douglasii* and *Quercus lobata* in California. *Ecology*, **73**, 2118–2128.

Callaway, R.M., DeLucia, E.H., Moore, D., Nowak, R. & Schlesinger, W.H. (1996) Competition and facilitation: contrasting effects of *Artemisia tridentata* on desert vs montane pines. *Ecology*, **77**, 2130–2141.

Chambers, J.C., Vander Wall, S.B. & Schupp, E.W. (1999) Seed and seedling ecology of pinon and juniper species in the pygmy woodlands of western North America. *Botanical Review*, **65**, 1–38.

Chapin, F.S., Randerson, J.T., McGuire, A.D., Foley, J.A. & Field, C.B. (2008) Changing feedbacks in the climate-biosphere system. *Frontiers in Ecology and the Environment*, **6**, 313–320.

Charney, J., Quirk, W.J., Chow, S.H. & Kornfield, J. (1977) Comparative study of effects of albedo change on drought in semi-arid regions. *Journal of the Atmospheric Sciences*, **34**, 1366–1385.

Cingolani, A.M., Vaieretti, M.V., Gurvich, D.E., Giorgis, M.A. & Cabido, M. (2010) Predicting alpha, beta and gamma plant diversity from physiognomic and physical indicators as a tool for ecosystem monitoring. *Biological Conservation*, **143**, 2570–2577.

Clifford, M.J., Rocca, M.E., Delph, R., Ford, P.L. & Cobb, N.S. (2008). Drought and bark beetle outbreak in Southwestern Pinyon-Juniper Woodlands. *Ecology, management, and restoration of piñon-juniper and ponderosa pine ecosystems: combined proceedings of the 2005 St. George, Utah and 2006 Albuquerque, New Mexico workshops.* (G.J. Gottfried, J.D. Shaw & P.L. Ford, compilers). pp. 39–51. Proceedings RMRS-P-51. US Department of Agriculture, Forest Service, Rocky Mountain Research Station, Fort Collins, CO, USA.

Conant, R.T., Klopatek, J.M., Malin, R.C. & Klopatek, C.C. (1998) Carbon pools and fluxes along an environmental gradient in northern Arizona. *Biogeochemistry*, **43**, 43–61.

Conant, R.T., Dalla-Betta, P., Klopatek, C.C. & Klopatek, J.A. (2004) Controls on soil respiration in semiarid soils. *Soil Biology & Biochemistry*, **36**, 945–951.

Davison, J.E., Breshears, D.D., van Leeuwen, W.J.D. & Casady, M.G. (2011) Remotely sensed vegetation phenology and productivity along a climatic gradient: on the value of incorporating the dimension of woody plant cover. *Global Ecology and Biogeography*, **20**, 101–113.

Eltahir, E.A.B. & Humphries, E.J. (1998) The role of clouds in the surface energy balance over the Amazon forest. *International Journal of Climatology*, **18**, 1575–1591.

Emerson, F.W. (1932) The tension zone between the grama grass and piñon-juniper associations in Northeastern New Mexico. *Ecology*, **13**, 347–358.

Everett, R.L., Koniak, S.K. & Budy, J.D. (1986) *Pinyon Seedling Distribution among Soil Surface Microsites*. USDA Forest Service. Research Paper INT-363. Intermountain Research Station, Ogden, UT.

Field, C.B., Lobell, D.B., Peters, H.A. & Chiariello, N.R. (2007) Feedbacks of terrestrial ecosystems to climate change. *Annual Review of Environment and Resources*, **32**, 1–29.

Floyd, M.L., Clifford, M., Cobb, N.S., Hanna, D., Delph, R., Ford, P. & Turner, D. (2009) Relationship of stand characteristics to drought-induced mortality in three Southwestern pinon-juniper woodlands. *Ecological Applications*, **19**, 1223–1230.

Gitlin, A.R., Sthultz, C.M., Bowker, M.A., Stumpf, S., Paxton, K.L., Kennedy, K., Munoz, A., Bailey, J.K. & Whitham, T.G. (2006) Mortality gradients within and among dominant plant populations as barometers of ecosystem change during extreme drought. *Conservation Biology*, **20**, 1477–1486.

Gruijter, J.J. & Braak, C.J.F. (1990) Model-free estimation from spatial samples: a reappraisal of classical sampling theory. *Mathematical Geology*, **22**, 407–415.

Gutschick, V.P. & BassiriRad, H. (2003) Extreme events as shaping physiology, ecology, and evolution of plants: toward a unified definition and evaluation of their consequences. *New Phytologist*, **160**, 21–42.

Huang, C.Y., Asner, G.P., Martin, R.E., Barger, N.N. & Neff, J.C. (2009) Multiscale analysis of tree cover and aboveground carbon stocks in pinyon-juniper woodlands. *Ecological Applications*, **19**, 668–681.

Huang, C.Y., Asner, G.P., Barger, N.N., Neff, J.C. & Floyd, M.L. (2010) Regional aboveground live carbon losses due to drought-induced tree dieback in pinon-juniper ecosystems. *Remote Sensing of Environment*, **114**, 1471–1479.

Isaaks, E.H. & Srivastava, R.M. (1989). *Applied Geostatistics*. Oxford University Press Inc, New York, 592 pp.

Jentsch, A., Kreyling, J. & Beierkuhnlein, C. (2007) A new generation of climate-change experiments: events, not trends. *Frontiers in Ecology and the Environment*, **5**, 365–374.

Madrigal-Gonzalez, J., Garcia-Rodriguez, J.A., Puerto-Martin, A., Fernandez-Santos, B. & Alonso-Rojo, P. (2010) Scale-dependent effects of pines on the herbaceous layer diversity in a semi-arid mediterranean ecosystem. *Community Ecology*, **11**, 77–83.

Maestre, F.T., Bautista, S. & Cortina, J. (2003) Positive, negative, and net effects in grass-shrub interactions in mediterranean semiarid grasslands. *Ecology*, **84**, 3186–3197.

Maestre, F.T., Callaway, R.M., Valladares, F. & Lortie, C.J. (2009) Refining the stress-gradient hypothesis for competition and facilitation in plant communities. *Journal of Ecology*, **97**, 199–205.

Martens, S.N., Breshears, D.D. & Meyer, C.W. (2000) Spatial distributions of understory light along the grassland/forest continuum: effects of cover, height, and spatial pattern of tree canopies. *Ecological Modelling*, **126**, 79–93.

McDowell, N.G., Allen, C.D. & Marshall, L. (2010) Growth, carbon-isotope discrimination, and drought-associated mortality across a Pinus ponderosa elevational transect. *Global Change Biology*, **16**, 399–415.

McDowell, N., Pockman, W.T., Allen, C.D., Breshears, D.D., Cobb, N., Kolb, T., Plaut, J., Sperry, J., West, A., Williams, D.G. & Yepez, E.A. (2008) Mechanisms of plant survival and mortality during drought: why do some plants survive while others succumb to drought? *New Phytologist*, **178**, 719–739.

Meagher, G.S. (1943) Reaction of piñon and juniper seedlings to artificial shade and supplemental watering. *Journal of Forestry*, **41**, 480–482.

Montes-Helu, M.C., Kolb, T., Dore, S., Sullivan, B., Hart, S.C., Koch, G. & Hungate, B.A. (2009) Persistent effects of fire-induced vegetation change on energy partitioning and evapotranspiration in ponderosa pine forests. *Agricultural and Forest Meteorology*, **149**, 491–500.

Notaro, M., Liu, Z. & Williams, J.W. (2006) Observed vegetation-climate feedbacks in the United States. *Journal of Climate*, **19**, 763–786.

Overpeck, J.T. & Cole, J.E. (2006) Abrupt change in Earth's climate system. *Annual Review of Environment and Resources*, **31**, 1–31.

Overpeck, J. & Udall, B. (2010) Dry times ahead. *Science*, **328**, 1642–1643.

Padien, D.J. & Lajtha, K. (1992) Plant spatial pattern and nutrient distribution in pinyon-juniper woodlands along an elevational gradient in northern New Mexico. *International Journal of Plant Sciences*, **153**, 425–433.

Pearcy, R.W., Ehleringer, J.R., Mooney, H. & Rundel, P.W. (1990) *Plant Physiological Ecology: Field Methods and Instrumentation*. Springer, New York.

Pongratz, J., Bounoua, L., DeFries, R.S., Morton, D.C., Anderson, L.O., Mauser, W. & Klink, C.A. (2006) The impact of land cover change on surface energy and water balance in Mato Grosso, Brazil. *Earth Interactions*, **10**, 1–17.

Raz-Yaseef, N., Rotenberg, E. & Yakir, D. (2010) Effects of spatial variations in soil evaporation caused by tree shading on water flux partitioning in a semi-arid pine forest. *Agricultural and Forest Meteorology*, **150**, 454–462.

Rich, P.M., Breshears, D.D. & White, A.B. (2008) Phenology of mixed woody-herbaceous ecosystems following extreme events: net and differential responses. *Ecology*, **89**, 342–352.

Rich, P.M., Dubayah, R., Hetrick, W.A. & Saving, S.C. (1994) Using viewshed models to calculate intercepted solar radiation: applications in ecology. *American Society for Photogrammetry and Remote Sensing Technical Papers*, pp. 524–529.

Rich, P.M., Wood, J., Vieglais, D.A., Burek, K. & Webb, N. (1999) *Guide to HemiView: Software for Analysis of Hemispherical Photography, Manual*. Delta-T Devices, Cambridge, UK.

Rotenberg, E. & Yakir, D. (2010) Contribution of semi-arid forests to the climate system. *Science*, **327**, 451–454.

Royer, P.D., Breshears, D.D., Zou, C.B., Cobb, N.S. & Kurc, S.A. (2010) Ecohydrological energy inputs in semiarid coniferous gradients: responses to management- and drought-induced tree reductions. *Forest Ecology and Management*, **260**, 1646–1655.

Scholes, R.J. & Archer, S.R. (1997) Tree-grass interactions in savannas. *Annual Review of Ecology and Systematics*, **28**, 517–544.

Selmants, P.C. & Hart, S.C. (2008) Substrate age and tree islands influence carbon and nitrogen dynamics across a retrogressive semiarid chronosequence. *Global Biogeochemical Cycles*, **22**, GB1021.

Shaw, J.D., Steed, B.E. & DeBlander, L.T. (2005) Forest Inventory and Analysis (FIA) annual inventory answers the question: what is happening to pinyon-juniper woodlands? *Journal of Forestry*, **103**, 280–285.

Smith, M.D. (2011) An ecological perspective on extreme climatic events: a synthetic definition and framework to guide future research. *Journal of Ecology*, **99**, 656–663.

Sthultz, C.M., Gehring, C.A. & Whitham, T.G. (2007) Shifts from competition to facilitation between a foundation tree and a pioneer shrub across spatial and temporal scales in a semiarid woodland. *New Phytologist*, **173**, 135–145.

Suarez, M.L. & Kitzberger, T. (2008) Recruitment patterns following a severe drought: long-term compositional shifts in Patagonian forests. *Canadian Journal of Forest Research-Revue Canadienne De Recherche Forestiere*, **38**, 3002–3010.

Villegas, J.C., Breshears, D.D., Zou, C.B. & Law, D.J. (2010a) Ecohydrological controls of soil evaporation in deciduous drylands: how the hierarchical effects of litter, patch and vegetation mosaic cover interact with phenology and season. *Journal of Arid Environments*, **74**, 595–602.

Villegas, J.C., Breshears, D.D., Zou, C.B. & Royer, P.D. (2010b) Seasonally pulsed heterogeneity in microclimate: phenology and cover effects along deciduous grassland-forest continuum. *Vadose Zone Journal*, **9**, 537–547. doi: 10.2136/vzj2009.0032.

Wang, L.X., D'Odorico, P., Manzoni, S., Porporato, A. & Macko, S. (2009) Soil carbon and nitrogen dynamics in southern African savannas: the effect of vegetation-induced patch-scale heterogeneities and large scale rainfall gradients. *Climatic Change*, **94**, 63–76.

Yaname, T. (1967) *Elementary Sampling Theory*. Prentince-Hall, Englewood Cliffs.

Zhao, M.S. & Running, S.W. (2010) Drought-induced reduction in global terrestrial net primary production from 2000 through 2009. *Science*, **329**, 940–943.

Zou, C.B., Barron-Gafford, G.A. & Breshears, D.D. (2007) Effects of topography and woody plant canopy cover on near-ground solar radiation: relevant energy inputs for ecohydrology and hydropedology. *Geophysical Research Letters*, **34**, L24S21.

Zou, C.B., Royer, P.D. & Breshears, D.D. (2010) Density-dependent shading patterns by Sonoran saguaros. *Journal of Arid Environments*, **74**, 156–158.

Received 16 August 2010; accepted 20 January 2011
Handling Editor: Alan Knapp

Supporting Information

Additional Supporting Information may be found in the online version of the article.

Table S1. Site description for tree cover and topography.

Table S2. Statistical table for analysis of variance.

Table S3. Statistical table for multiple regression analysis.

Figure S1. A study area map.

Figure S2. Site climate data.

Figure S3. Workflow diagram.